Influence of the latitudinal temperature gradient on soil dust concentration and deposition in Greenland

Ina Tegen[1]
Department of Applied Physics, Columbia University, New York

David Rind
NASA Goddard Institute for Space Studies, New York

Abstract

To investigate the effects of changes in the latitudinal temperature gradient and the global mean temperature on dust concentration in the Northern Hemisphere, experiments with the GISS GCM are performed. The dust concentration over Greenland is calculated from sources in central and eastern Asia, which are integrated on-line in the model. The results show that an increase in the latitudinal temperature gradient increases both the Asian dust source strength and the concentration over Greenland. The source increase is the result of increased surface winds, and to a minor extent, the increase in Greenland dust is also associated with increased northward transport. Cooling the climate in addition to this increased gradient leads to a decrease in precipitation scavenging, which helps produce a further (slight) increase in Greenland dust in this experiment. Reducing the latitudinal gradient reduces the surface wind and hence the dust source, with a subsequent reduction in Greenland dust concentrations. Warming the climate in addition to this reduced gradient leads to a further reduction in Greenland dust due to enhanced precipitation scavenging. These results can be used to evaluate the relationship of Greenland ice core temperature changes to changes in the latitudinal and global temperatures.

dient and the changes in the average temperature may cause a change in the dust signal in Greenland by changes in wind speeds, precipitation, or changes in circulation patterns. In an attempt to distinguish these alternatives, in this paper we investigate the consequences of such changes on dust concentrations at Greenland. This follows an investigation by *Rind* [1998], who evaluated the effects of a change in the latitudinal sea surface temperature (SST) gradient using the Goddard Institute for Space Studies (GISS) GCM. (Here we do not attempt to use a GCM to simulate all of the possible processes involved in creating the strong dust signal in Greenland, since many boundary conditions responsible for dust deflation during different climate periods like soil surface conditions are difficult to constrain.) If changes in dust transport to Greenland can be attributed to either changes in temperature gradient or changes in global average temperatures, we might be able to infer changes in the latitudinal temperature gradient from the observed Greenland dust records. This may give an additional indication whether the temperature gradient information we can obtain from the limited amount of ice records in the Northern Hemisphere (NH) is sufficient to reconstruct the hemispherical temperature conditions. This investigation is specifically of interest for time periods where land surface conditions, which could potentially affect dust deflation, did not change considerably (vegetation changes or addition of glacial outwash), since those changes were not included in the simulation.

2. Dust As Tracer in the GISS GCM

Dust has been included as a dynamic tracer in the GISS atmospheric GCM (4° × 5°horizontal resolution, nine vertical layers). This parameterization and some results thereof have been described by *Tegen and Miller* [1998]. Dust sources, transport, and deposition were computed with a 1-hour time step. In the GCM, dust emissions are computed as a function of vegetation cover, surface wind speed, and soil moisture [*Tegen and Fung,* 1994]. Dust deflation is allowed in areas labeled by *Matthews* [1983] as deserts or sparsely vegetated regions. The GCM transports four size classes of dust, with size ranges of 0.1-1, 1-2, 2-4, and 4-8 μm as independent tracers. Sizes below 1 μm were transported as one size class because they are not strongly fractionated by gravitational settling. Particle sizes larger than 8 μm were not included in this calculation, since large particles fall out quickly and are not important for long-range dust transport.

Surface distributions of clay (particles smaller than 1 μm) and small silt (particle radius between 1 and 10 μm) were derived from a global soil texture data set [*Zobler,* 1986; *Webb et al.,* 1991]. Measurements show that above a critical threshold velocity (below which no dust deflation takes place), dust fluxes into the atmosphere depend on the third power of surface wind speed [*Gillette,* 1978] which is the most critical parameter for calculating dust emissions on the global scale. In the model the dust flux in those areas, where the surface conditions allow dust deflation, follows

$$q_a = C(u - u_{tr})u^2, \qquad (1)$$

where q_a is the dust flux from the surface in μg m^{-2} s^{-1}, u is the surface wind speed in m s^{-1}, and u_{tr} is a threshold velocity. For wind speeds below this threshold, no dust deflation takes place. We used the dimensional constant of $C = 2$ μg s^2 m^{-5} for clay particles (< 1 μm) and $C = 5$ μg s^2 m^{-5} for silt particles (1-8 μm) to describe dust deflation [*Tegen and Miller,* 1998]. Because the dust emissions increase nonlinearly with surface wind speed, peak wind speed events are responsible for a major part of dust deflation. High-wind events in the GCM are less frequent compared to the previously used European Centre for Medium-Range Weather Forecasts (ECMWF) surface-wind products with a spatial resolution of 1.125° × 1.125° [*Tegen and Fung,* 1994]. This leads to an underestimate of dust emissions in the GCM experiments. To reduce this difference, we chose a threshold velocity for each land grid box in the GCM that results in the same dust fluxes compared to the off-line model with ECMWF surface winds (for which the threshold velocity was 6.5 m s^{-1} at all locations) [*Tegen and Fung,* 1995]. The resulting threshold velocities for GCM surface wind speed vary between 4 and 10 m s^{-1}. We chose to vary the threshold velocities at each gridbox instead of varying the emission factor, because this way the number of dust events occurring per year at each gridbox would be similar to the off-line results that used the ECMWF surface wind product.

Dust is removed from the atmosphere by gravitational settling using Stokes law (size-dependent settling velocities), turbulent mixing in the first model layer, and subcloud washout calculated using GCM precipitation. A detailed description of this parameterization and the validation of the results under present-day conditions can be found in the work of *Tegen and Miller* [1998]. For these experiments, only Asian dust sources are included; that is, dust fluxes

pared with the standard deviation than the increase in dust concentrations by the increase in the SST gradient. Figure 3 shows for case B similar concentrations near the source areas compared to the control case 0, but the concentrations over North America of dust transported eastward from Asia are smaller; that is, in this case, less dust is transported away from the source region. The response of dust concentrations to changes in the SST gradient is therefore not symmetrical, the sign of the change in the gradient does influence the strength in the dust response.

An additional decrease in global average SST together with the increased temperature gradient (experiment C) further increases the dust concentration at Greenland. However, the increase in the SST gradient (experiment A) increases the overall dust concentrations stronger compared to the control experiment than a decrease in global average SSTs alone. This becomes clear when considering the effect of SST decrease alone by subtracting the results of experiment C from experiment A (Figure 3, top middle panel). For this case, the concentration of dust above Asia is of the same order of magnitude as for the control case (experiment 0), but the dust is transported farther across North America. For experiment C the combination of these effects results in dust concentrations near the Asian source areas being similar to case A but also in slightly increased dust transport and concentration over North America and Greenland. There, the dust concentration in experiment C is $\approx$ 20% higher than for experiment A (see Table 1). This additional increase in Greenland dust is less significant than the increase of dust in experiment A compared to the control case, considering the large standard deviation.

For the opposite case, if the global mean temperatures are increased additionally to a decrease in latitudinal temperature gradient (experiment D), the dust concentration at Greenland is further reduced by about 30% compared to experiment B (Table 1). If only the effect of changes in global SST is considered compared to the change in the SST gradient only (by subtracting the results from experiment B from experiment D, middle panel in Figure 3), the dust concentrations over both Asian source areas and dust transport across North America are slightly reduced compared to the control experiment. For case D this change, together with the change due to the decrease in SST gradient, leads to a noticeable reduction of dust concentrations over the source areas and the dust transported eastward.

Because soil-surface conditions (e.g., changes in vegetation cover or land ice) did not change in these calculations, dust concentration changes can be caused by either changes in dust source strengths or changes in transport. Such changes, in turn, can be caused by changes in surface wind speed, changes in wind direction, or changes in precipitation, which can impact both washout rate of the dust during its transport and soil moisture in the source region, changing the source strength of dust.

3.3. Changes in Dust Source Strengths

Table 1 also summarizes the dust source strengths for the different GCM experiments. For increased SST gradients the source strength for eastern Asian (China) sources is increased by a factor of 3 compared to the control experiment, while the central Asian source is increased by a factor of $\approx$ 2. This corresponds well to the factor 2-3 increase in dust concentrations over Greenland for this case. On the other hand, a decrease in the SST gradient (case B) does not lead to a significant decrease in dust source strengths in Asia, as would have been expected if the response of the dust to the SST gradient change had been symmetrical.

For experiment C the eastern and central Asian source strengths of dust do not increase with an additional decrease in global mean SSTs, in fact, they are slightly lower than for experiment A. This indicates that for an increased gradient the increase in dustiness at Greenland is controlled by changes in the dust source strength, assuming the transport path is the same as in the control experiment. With additional colder temperatures the additional increase in Greenland dust must be caused by changes in transport or dust deposition. For the opposite case, an increase in global SSTs in addition to a decreased SST gradient (case D) leads to an $\approx$ 30% decrease in central Asian dust sources compared to case B (increased SST gradient only), while the Chinese dust sources remain effectively unchanged. This decrease is small compared to the standard deviation, however.

This change in dust source strength can be caused by changes in surface wind speed, which influences the dust deflation, or by changes in precipitation and soil moisture, which determines whether a given gridbox can act as a dust source (if the vegetation cover allows for dust deflation). Plates 1a-i show difference maps for the dust source strengths, surface wind speed, and precipitation for experiment A minus experiment B (the difference between the experiments

dust concentrations found in Greenland for the GCM integrations with changed average SSTs compared to changed latitudinal temperature gradients (Table 1), while differences in the dust source strengths cannot explain this difference (comparison of experiments A and C).

Dust transport may be affected not only by changes in the removal rates but also by changes in transport pathways. Northward dust transports for experiments A - D and control experiment 0 are shown in Figure 4 for the zonal mean. To compare the differences in the transport without including the changes in dust source strength and removal rates, the values for northward dust transport were divided by the total dust content of the atmosphere for each experiment. The northward transport of dust does not considerably change for the different SST boundary conditions. For experiment A (increased SST gradient) the northward dust transport between $\approx 40°$ and 70°N increases compared to the control experiment, for experiment C (additional cooling) there is only a small increase in northward dust transport compared to the control experiment. The changes in Greenland dust concentrations in the other experiments can therefore be explained by changes in source strengths due to changes in zonal wind speed and by changes in washout rates due to changes in precipitation strengths alone. For the increased temperature gradient (without changes in the global mean SST) an increase in northward transport also may be a factor causing the increased dust in Greenland. However, since for this case the factor of increase in Greenland dust concentrations agrees well with the factor of increase in dust source strength (see Table 1), we conclude that the changes in dust transport pathways are of comparatively minor importance.

3.5. Changes in Dust Deposition

The deposition of dust at Greenland is of interest, since the dust signal in ice cores reflects changes in the deposited dust on the ground rather than airborne dust concentrations at the ice core site. However, as mentioned above, the model underestimates the precipitation at Greenland and therefore overestimates dust concentrations in precipitation and may underestimate dust deposition fluxes at this location. Table 2 shows total and wet dust deposition at the GISP site for the GCM experiments together with the annual precipitation and annual mean dust concentration in precipitation (based on monthly averages). The wet deposition at this site is only about 50% of the total (wet plus dry) deposition for cases A and C, 60% for the control experiment, and $\approx$ 70% for cases B and D. This reflects the differences in precipitation in the model, which is by a factor of 2 smaller for the colder climate (experiment C), and by a factor of 2 higher for the warmer climate (experiment D) compared to the control experiment: for higher precipitation rates the wet deposition dominates the dry deposition at this remote location. Generally, dust deposition for the different GCM experiments follows the trend for dust concentrations, where the increase in SST gradient (experiment A) leads to an increase by a factor of $\approx$ 2-2.5 in the dust deposition (and concentration in precipitation), while the deposition flux for experiment C is not significantly higher than for case A. On the other hand, the dust concentration in precipitation is 30% higher for case C, which is due to the differences in the precipitation. The experiments with the decreased SST gradient also show a similar trend for deposition fluxes as the dust concentrations at Greenland, with the total deposition fluxes being about a factor of 2 smaller compared to the control run. These results indicate that even with the differences in precipitation at the Greenland location, the changes in deposition fluxes are similar to the changes in dust concentrations at this location.

3.6. Spring Conditions

As mentioned above, the dust signal at Greenland in the GCM shows a summer maximum, although the Asian dust source has a spring maximum. This discrepancy may be due to a high-latitude source that is active in the NH summer. Even though Asian sources north of 50°N contribute less than 10% and sources north of 60°N contribute less than 1% to the total Asian dust emission, such sources may disproportionally influence dust concentrations in Greenland. No measurements exist to prove or disprove the existence of a dust source at those high-latitude locations. Because of lack of measurements the existence of such a dust source cannot be excluded.

To evaluate whether the results presented here are still valid for the case that the model did incorrectly predict the existence of such a high-latitude Asian source, we investigated the GCM results for NH spring additionally to the annual averages. During NH spring the high-latitude Siberian source is not active, while dust emissions in Asia are largest. Table 3 summarizes the results for the Asian dust sources and Greenland dust concentration for NH spring. For case A, the increase in springtime dust concentration

tributed to greater dust concentrations, although gradient changes of the values given here were not sufficient to produce the order of magnitude increase found in the GISP ice core. Other obvious differences that were not taken into account in these calculations could explain these differences: changes in surface conditions (glacial outwash and vegetation decrease) would be expected to fundamentally increase the dust source strengths in Asia and subsequent transport to Greenland. Furthermore, the existence of large land ice sheets in the Northern Hemisphere could well have altered circulation patterns. Only a specific simulation with these boundary condition changes can act to provide a full assessment of the magnitude of the latitudinal gradient change applicable to the LGM.

Acknowledgments. This work was supported by the National Oceanic and Atmospheric Administration (NOAA grant NA56GP0450). We thank Dr. M. Prentice and an anonymous reviewer for useful discussions.

References

Andersen, K. K., A. Armengaud, and C. Genthon, Atmospheric dust under glacial and interglacial conditions, *Geophys. Res. Lett.*, *25*, 2281–2284, 1998.

Biscaye, P. E., F. E. Grousset, M. Revel, S. Van der-Gaast, G. A. Zielinski, A. Vaara, and G. Kukla, Asian provenance of glacial dust (stage 2) in the Greenland Ice Sheet Project 2 Ice Core, Summit, Greenland, *J. Geophys. Res.*, *102*, 26,765–26,781, 1997.

Cuffey, K. M., and D. G. Clow, Temperature, accumulation, and ice sheet elevation in central Greenland through the last deglacial transition, *J. Geophys. Res.*, *102*, 26,383–26,396, 1997.

Davidson, C. I., et al., Chemical constituents in the air and snow at Dye 3, Greenland I, Seasonal variations, *Atmos. Environ.*, *27*A, 2709–2722, 1993.

Gao, Y., R. Arimoto, J. T. Merril, and R. A. Duce, Relationships between the dust concentrations over eastern Asia and the remote North Pacific, *J. Geophys. Res.*, *97*, 9867–9872, 1992.

Genthon, C., Simulations of the long-range transport of desert dust and sea salt in a general circulation model, in *Precipitation Scavenging and Atmosphere-Surface Exchange*, edited by S. E. Schwartz and W. G. N. Slinn, pp. 1783–1794, Hemisphere Publ., Washington, D.C., 1992.

Gillette, D., A wind tunnel simulation of the erosion of soil: Effect of soil texture, sandblasting, wind speed, and soil consolidation on dust production, *Atmos. Environ.*, *12*, 1735–1743, 1978.

Joussaume, S., Paleoclimate tracers: An investigation using an atmospheric general circulation model under ice age conditions, 1, Desert dust, *J. Geophys. Res.*, *98*, 2767–2805, 1993.

Jouzel, J., et al., Validity of the temperature reconstruction from water isotopes in ice cores, *J. Geophys. Res.*, *102*, 26,471–26,487, 1997.

Kahl, J. D., A. M. Dewayne, H. Kuhns, C. I. Davidson, J. Jaffrezo, and J. M. Harris, Air mass trajectories to Summit, Greenland: A 44-year climatology and some episodic events, *J. Geophys. Res.*, *102*, 26,861–26,875, 1997.

Legrand, M., Atmospheric chemistry changes versus past climate inferred from polar ice cores, in *Aerosol Forcing of Climate*, edited by R. Charlson and J. Heintzenberg, pp. 123–152, John Wiley, New York, 1995.

Littmann, T., Dust storm frequency in Asia: Climatic control and variability, *Int. J. Climatol.*, *11*, 393–412, 1991.

Matthews, E., Global vegetation and land use: New high-resolution databases for climate studies, *J. Clim. Appl. Meteorol.*, *22*, 474–487, 1983.

Mayewski, P. A., L. D. Meeker, M. C. Morrison, M. S. Twickler, S. Whitlow, K. K. Ferland, D. A. Meese, M. R. Legrand, and J. P. Steffensen, Greenland ice core "signal" characteristics: An expanded view of climate change, *J. Geophys. Res.*, *98*, 12,839–12,847, 1993.

Mayewski, P. A., et al., Changes in atmospheric circulation and ocean ice cover over the North Atlantic during the last 41,000 years, *Science*, *263*, 1747–1751, 1994.

Mosher, B. W., P. Winkler, and J. L. Jaffrezo, Seasonal aerosol chemistry at Dye 3, Greenland, *Atmos. Environ.*, *27*A, 2761–2772, 1993.

Mosley-Thompson, E., L. G. Thompson, J. Dai, M. Davis, and P. N. Lin, Climate of the last 500 years: High resolution ice core records, *Quat. Sci. Rev.*, *12*, 419–430, 1993.

O'Brien, S. R., P. A. Mayewski, L. D. Meeker, D. A. Meese, M. S. Twickler, and S. I. Whitlow, Complexity of Holocene climate as reconstructed from a Greenland ice core, *Science*, *270*, 1962–1964, 1995.

Pye, K., *Aeolian Dust and Dust Deposits*, Academic, San Diego, Calif., 1987.

Rea, D. K., The paleoclimatic record provided by eolian deposition in the deep sea: The geologic history of wind, *Rev. Geophys.*, *32*, 159–195, 1994.

Figure 1. Seasonal mixing ratios (in μg dust/kg air) of Asian dust aerosol for the control experiment 0 for the first model layer.

Figure 2. Seasonality of dust at Greenland for the control experiment 0 for deposition (in mg m^{-2} d^{-1}), first layer concentration (in $\mu g/m^3$), dust concentration in precipitation (in mg/kg water), and precipitation (in mm d^{-1}).

Figure 3. Annually and vertically averaged dust mixing ratios for experiments A-D and control experiment 0, together with dust concentrations for only decreased (C-A+0) or increased (D-B+E) global SSTs (in μg dust/kg air).

Figure 4. Zonal mean northward dust transports for experiments A-D and control experiment 0, relative to the total dust content of the atmosphere.

Plate 1. Differences in dust sources (a,b,c), zonal wind speeds (d,e,f), and precipitation (g,h,i) for changes in the latitudinal SST gradient (experiment A minus experiment B) (a,d,g), colder conditions without changes in the temperature gradient (experiment C minus experiment A) (b,e,h), and warmer conditions without changes in the temperature gradient (experiment D minus experiment B) (c,f,i).

Figure 1. Seasonal mixing ratios (in μg dust/kg air) of Asian dust aerosol for the control experiment 0 for the first model layer.

Figure 2. Seasonality of dust at Greenland for the control experiment 0 for deposition (in mg m^{-2} d^{-1}), first layer concentration (in $\mu g/m^3$), dust concentration in precipitation (in mg/kg water), and precipitation (in mm d^{-1}).

Figure 3. Annually and vertically averaged dust mixing ratios for experiments A-D and control experiment 0, together with dust concentrations for only decreased (C-A+0) or increased (D-B+E) global SSTs (in μg dust/kg air).

Figure 4. Zonal mean northward dust transports for experiments A-D and control experiment 0, relative to the total dust content of the atmosphere.

Plate 1. Differences in dust sources (a,b,c), zonal wind speeds (d,e,f), and precipitation (g,h,i) for changes in the latitudinal SST gradient (experiment A minus experiment B) (a,d,g), colder conditions without changes in the temperature gradient (experiment C minus experiment A) (b,e,h), and warmer conditions without changes in the temperature gradient (experiment D minus experiment B) (c,f,i).

Table 2. GCM Results for Annual Average Precipitation and Dust Deposition at Greenland

	Depos. Flux $mg/m^2/yr$	Depos. Flux (Wet) $mg/m^2/yr$	Precipitation mm/yr	Conc. (Precip.) $\mu g/kg$ Water
C (A + colder)	52 ± 10	22 ± 5	36 ± 9	490 ± 110
A (increased gradient)	51 ± 12	23 ± 7	57 ± 16	380 ± 90
0 (control)	22 ± 6	14 ± 4	83 ± 22	160 ± 58
B (decreased gradient)	12 ± 3	8 ± 3	98 ± 23	79 ± 22
D (B + warmer)	10 ± 3	7 ± 3	150 ± 30	53 ± 18

Table 3. GCM Results for Dust Sources and Dust Concentrations at Greenland for NH Spring

	China Source $mg/m^2/yr$	Central Asia Source $mg/m^2/Seas$	Conc. (Layer 1) $\mu g/m^3$	Avg Mixing Ratio $\mu g/kg$ Air
C (A + colder)	5.3 ± 2.6	20 ± 8	0.71 ± 0.11	1.6 ± 0.2
A (increased gradient)	$13. \pm 5.$	31 ± 10	1.1 ± 0.24	2.2 ± 0.3
0 (control)	$3.7 \pm 2.$	15 ± 6	0.27 ± 0.09	0.9 ± 0.2
B (decreased gradient)	$3. \pm 1.8$	8 ± 4	0.16 ± 0.04	0.6 ± 0.1
D (B + warmer)	1.8 ± 1	7 ± 3	0.10 ± 0.03	0.5 ± 0.1

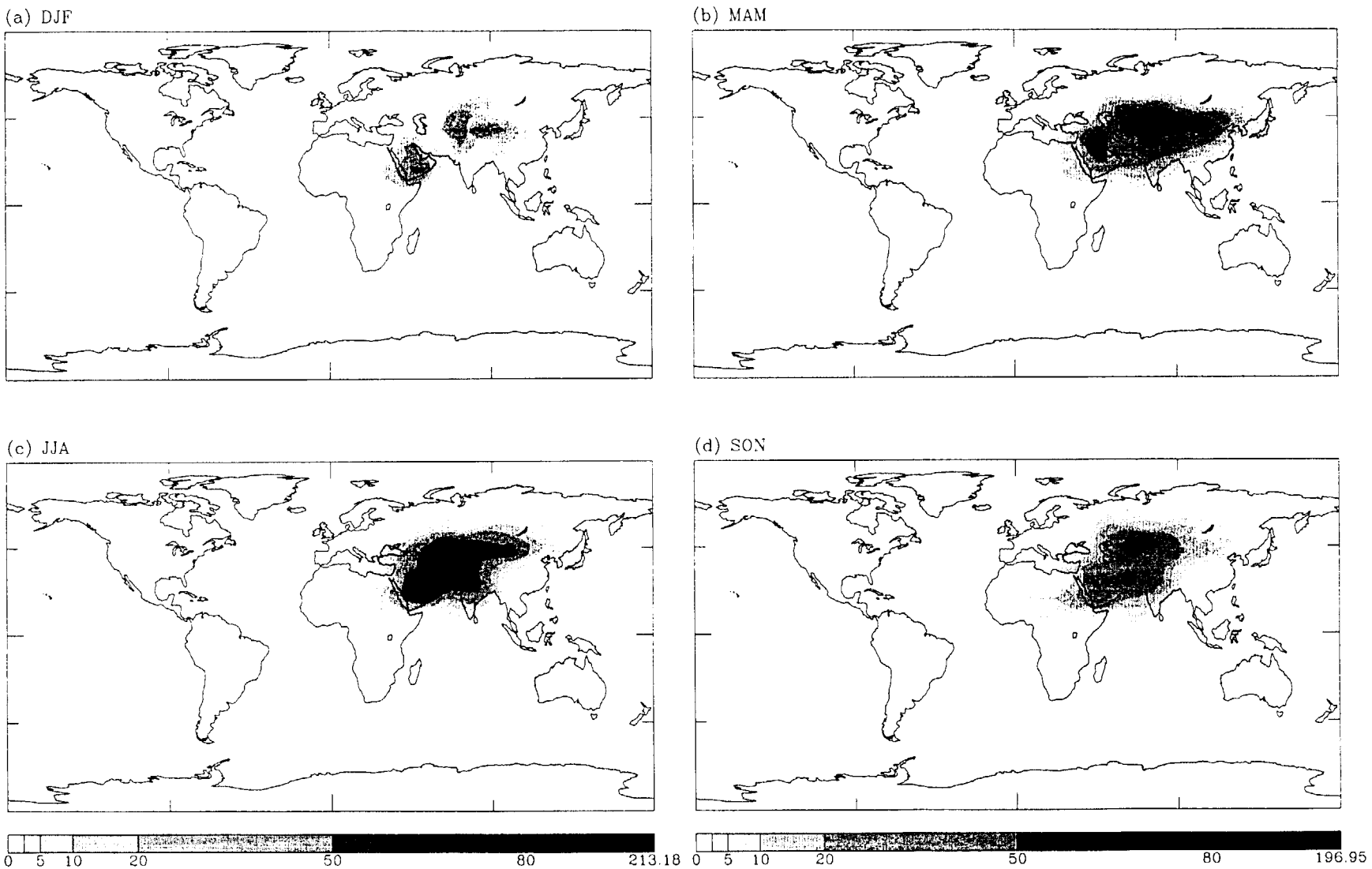
1st Layer Dust Concentration
(μg dust/kg air)
CONTROL
(a) DJF
(b) MAM
(c) JJA
(d) SON
0 5 10 20 50 80 213.18
0 5 10 20 50 80 196.95

Figure 1

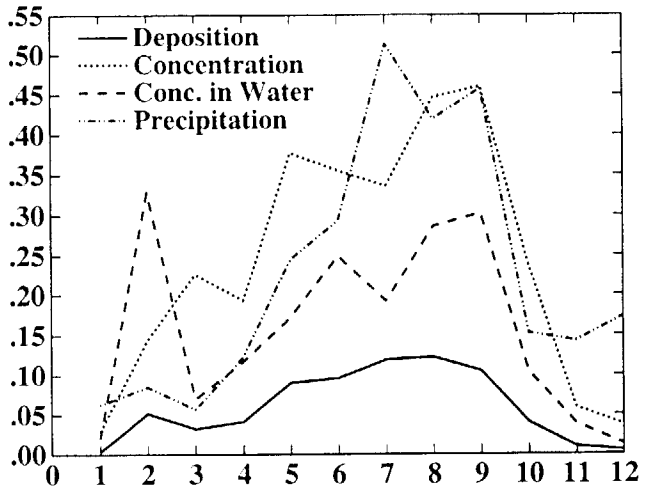
Deposition
Concentration
Conc. in Water
Precipitation
.55
.50
.45
.40
.35
.30
.25
.20
.15
.10
.05
.00
0 1 2 3 4 5 6 7 8 9 10 11 12
Month

Figure 2

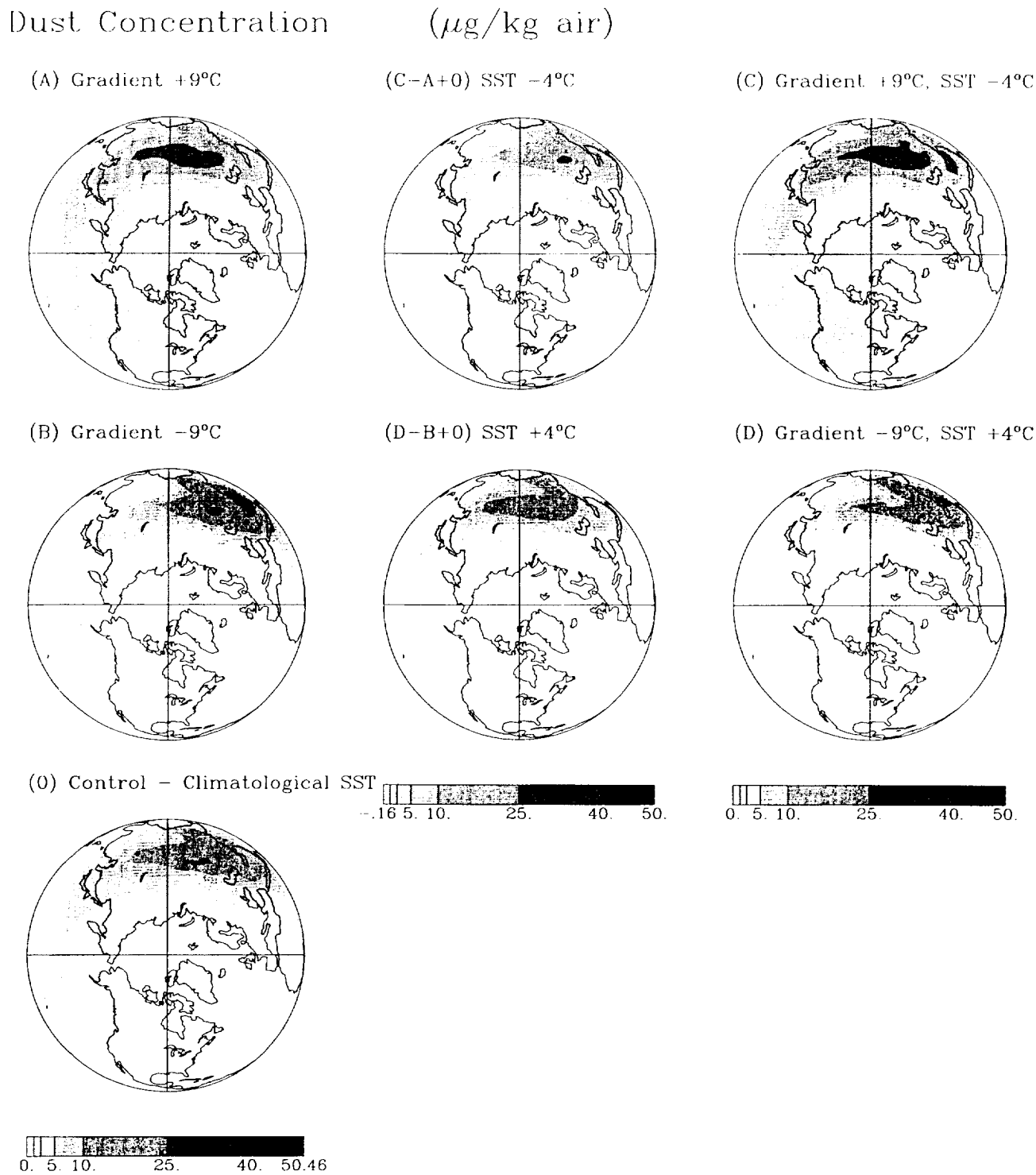
Dust Concentration (μg/kg air)
(A) Gradient +9°C
(C-A+0) SST -4°C
(C) Gradient +9°C, SST -4°C
(B) Gradient -9°C
(D-B+0) SST +4°C
(D) Gradient -9°C, SST +4°C
(0) Control - Climatological SST
-.16 5. 10. 25. 40. 50.
0. 5. 10. 25. 40. 50.
0. 5. 10. 25. 40. 50.46

Figure 3

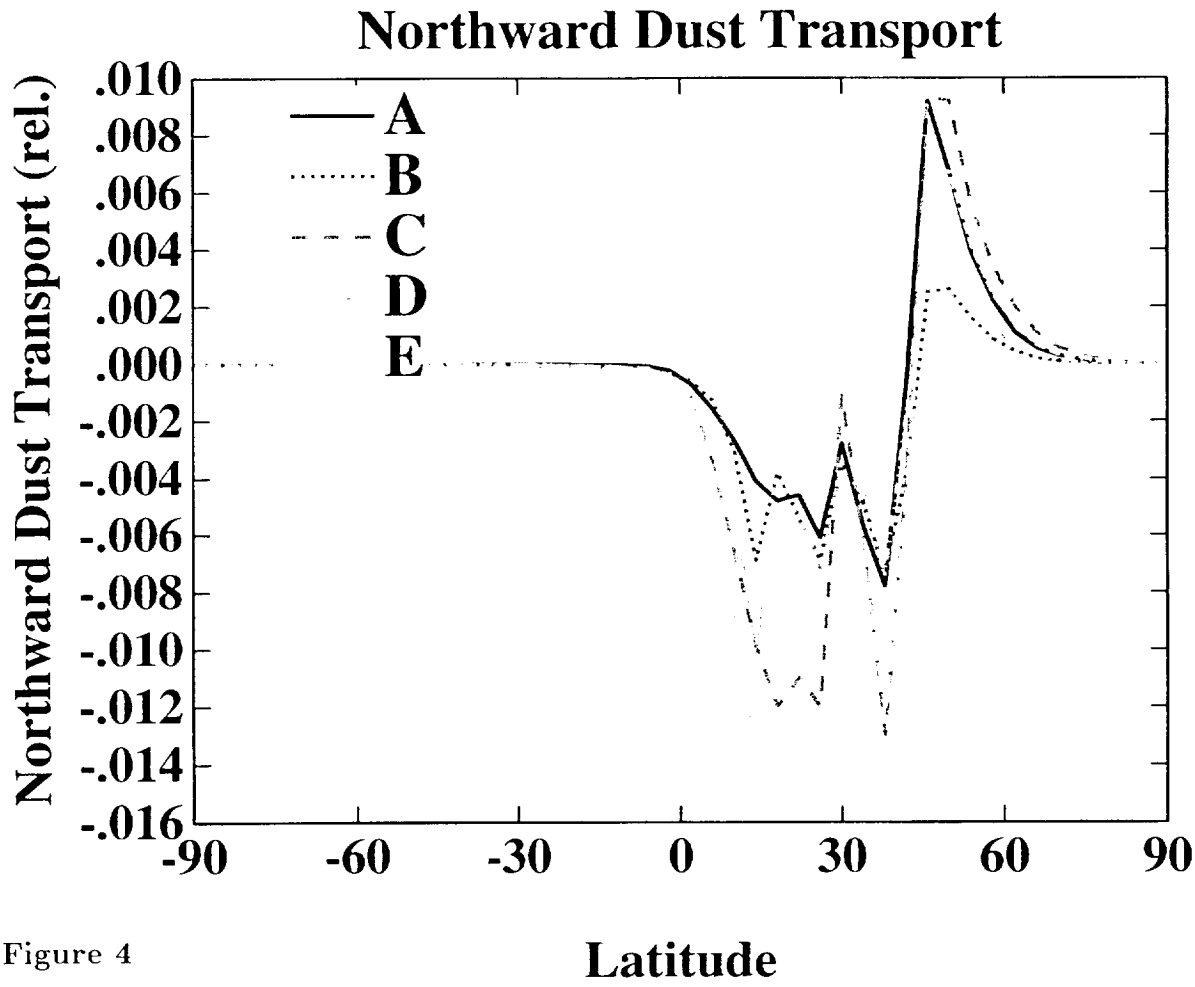
Northward Dust Transport
Northward Dust Transport (rel.)
.010
.008
.006
.004
.002
.000
-.002
-.004
-.006
-.008
-.010
-.012
-.014
-.016
A
B
C
D
E
-90
-60
-30
0
30
60
90
Latitude

Figure 4

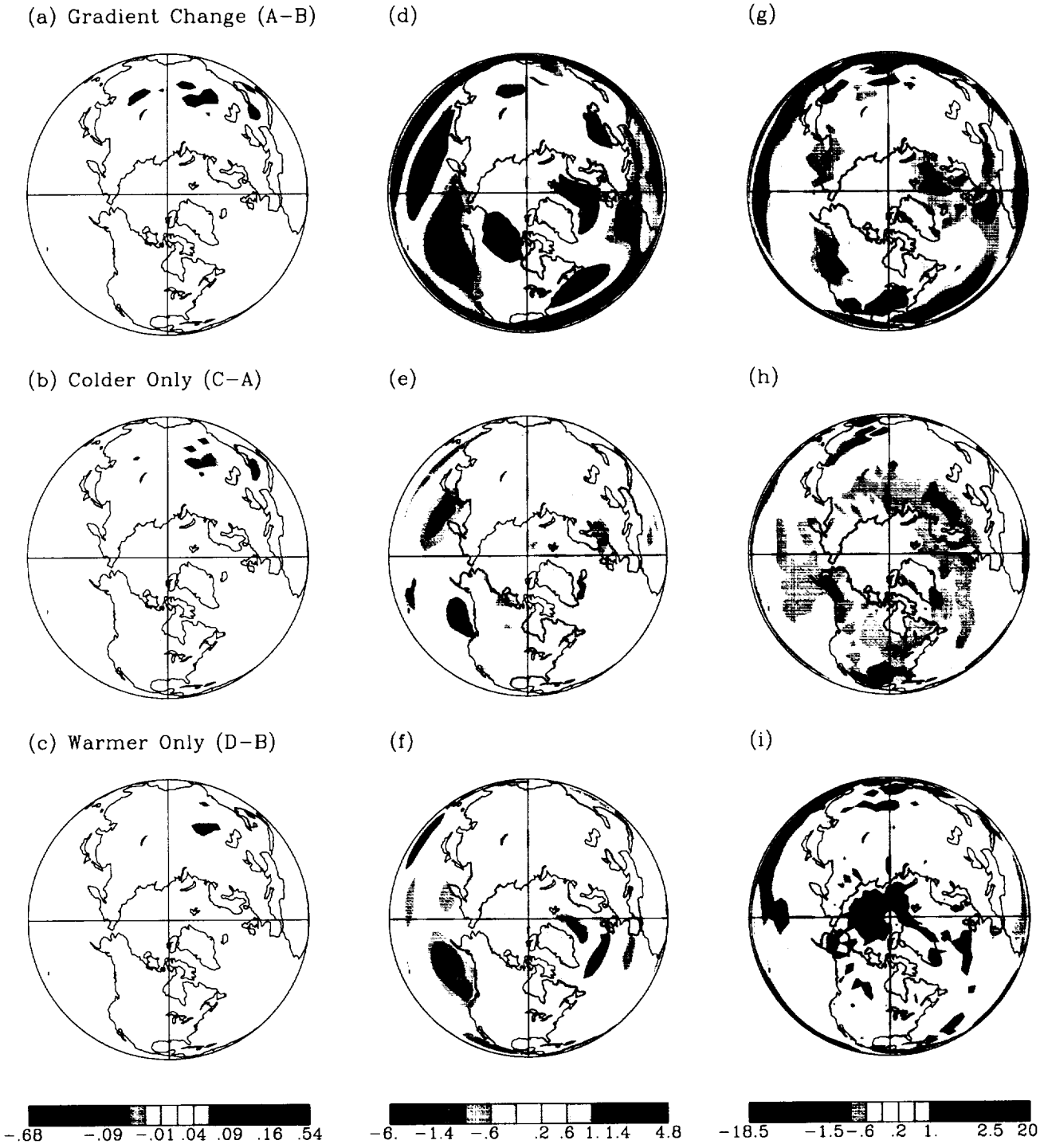
Dust Flux (g/m²/d)
Zonal Surface Wind (m/s)
Precipitation (mm/d)
(a) Gradient Change (A−B)
(d)
(g)
(b) Colder Only (C−A)
(e)
(h)
(c) Warmer Only (D−B)
(f)
(i)
−.68 −.09 −.01 .04 .09 .16 .54
−6. −1.4 −.6 .2 .6 1. 1.4 4.8
−18.5 −1.5 −.6 .2 1. 2.5 20.